



Article

Variability of Antarctic sea ice extent over the past 200 years

Jiao Yang^a, Cunde Xiao^{b,*}, Jiping Liu^c, Shutong Li^{a,d}, Dahe Qin^{a,*}

^aState Key Laboratory of Cryospheric Science, Northwest Institute of Eco-Environment and Resources, Chinese Academy of Sciences, Lanzhou 730000, China

^bState Key Laboratory of Earth Surface Processes and Resource Ecology, Beijing Normal University, Beijing 100875, China

^cDepartment of Atmospheric and Environmental Sciences, University at Albany, State University of New York, Albany NY 12222, USA

^dCollege of Resources and Environment, University of Chinese Academy of Sciences, Beijing 100049, China

ARTICLE INFO

Article history:

Received 25 November 2020

Received in revised form 3 July 2021

Accepted 5 July 2021

Available online 21 July 2021

Keywords:

Antarctic

Sea ice

Ice core

Southern Annular Mode

Interdecadal Pacific Oscillation

ABSTRACT

While Arctic sea ice has been decreasing in recent decades that is largely due to anthropogenic forcing, the extent of Antarctic sea ice showed a positive trend during 1979–2015, followed by an abrupt decrease. The shortness of the satellite record limits our ability to quantify the possible contribution of anthropogenic forcing and internal variability to the observed Antarctic sea ice variability. In this study, ice core and fast ice records with annual resolution from six sites are used to reconstruct the annual-resolved northernmost latitude of sea ice edge (NLSIE) for different sectors of the Southern Ocean, including the Weddell Sea (WS), Bellingshausen Sea (BS), Amundsen Sea (AS), Ross Sea (RS), and the Indian and western Pacific Ocean (IndWPac). The linear trends of the NLSIE are analyzed for each sector for the past 100–200 years and found to be -0.08° , -0.17° , $+0.07^\circ$, $+0.02^\circ$, and -0.03° per decade ($\geq 95\%$ confidence level) for the WS, BS, AS, RS, and IndWPac, respectively. For the entire Antarctic, our composite NLSIE shows a decreasing trend (-0.03° per decade, 99% confidence level) during the 20th century, with a rapid decline in the mid-1950s. It was not until the early 1980s that the observed increasing trend occurred. A comparison with major climate indices shows that the long-term linear trends in all five sectors are largely dominated by the changes in the Southern Annular Mode (SAM). The multi-decadal variability in WS, BS, and AS is dominated by the Interdecadal Pacific Oscillation, whereas that in the IndWPac and RS is dominated by the SAM.

© 2021 Science China Press. Published by Elsevier B.V. and Science China Press. All rights reserved.

1. Introduction

Sea ice has important effects on local and regional climate variability through multiple processes. For example, sea ice modulates the transfer of moisture and heat between oceans and the atmosphere. Satellite observations have shown that sea ice in the Arctic has been declining rapidly over the last 40 years, which is consistent with the expectation of amplified Arctic warming due to ice-albedo feedback [1,2]. In contrast, the total sea ice extent (SIE) in the Antarctic showed a slight but significantly increasing trend from 1979 to 2015, although this trend did not continue in recent years (2016–2018), during which anomalously low ice cover was observed [3]. At the regional scale, the SIE of the Ross Sea in winter, summer, and autumn and that of the Weddell Sea in summer and autumn have shown positive trends, whereas negative trends are dominant in the western Weddell Sea in winter and in the Amundsen/Bellingshausen Seas in summer and autumn [3–5]. Coupled climate models have had limited success in correctly simulating

fundamental aspects of the observed annual cycle and the long-term trends [3,6,7]. The discrepancy between climate models and observations likely stems from climate forcing, rather than sea ice physics [7,8].

Multiple factors contribute to the observed trends of Antarctic SIE [9,10]. Several mechanisms have been proposed to explain the weakly positive trend in the Antarctic SIE. Multi-decadal modulations of sea surface temperature (SST) in the tropical Pacific and north Atlantic may strengthen the Amundsen Sea Low and cyclone activities [11–15]. The freshened ocean surface, which reduces the upwelling of warmer subsurface waters, might also increase Antarctic sea ice cover [16–18]. The cooling of surface waters in the Southern Ocean due to the observed strengthening of the westerly winds and upward trend in the Southern Annular Mode (SAM) might be another factor resulting in the positive trend in Antarctic SIE [19,20]. The rapid decrease that began in 2016 had been associated with anomalous atmospheric conditions tele-connected with the warming in the eastern Indian Ocean and a negative SAM [21–25]. However, there is no consensus on the cause of the observed changes.

* Corresponding authors.

E-mail addresses: cdxiao@bnu.edu.cn (C. Xiao), qdh@cma.gov.cn (D. Qin).

The satellite data record in the Antarctic is quite short; it begins in the late 1970s, and the discrepancies between observations and model simulations limit our understanding of Antarctic sea ice variability and its links to regional climate over longer periods, especially at the multi-decadal scale [10,26,27]. Climate model simulations of future warming are heavily dependent on the historical sea ice area data [28], and it is therefore critical to provide reliable reconstructed paleo-sea ice data to ensure that the climate models tasked with predicting future changes are fully optimized [29].

Using paleoclimate archives is the best approach for reconstructing the past sea ice state. Several studies have reconstructed past changes in Antarctic sea ice using various proxy data extracted from ice cores [30–36]. They have linked a number of chemical species (e.g., methane sulphonic acid (MSA) [37,38], sea salt sodium [36,39], and deuterium excess [40]) to the sea ice changes around Antarctica. These studies have suggested that the winter SIE in the western Pacific and Indian Ocean sectors has declined since the 1950s [30,34]. In contrast, the winter SIE in the Ross Sea has concurrently demonstrated an increasing trend, with the largest increase observed after the early 1990s [35,40]. During the 20th century, the sea ice in the Amundsen and Ross seas expanded $\sim 1^\circ$ northward [35], while the Indian Ocean sector [34] and the Bellingshausen Sea [32] experienced a significant sea ice retreat [29,41]. When a longer time scale is considered, it is observed that the Indian Ocean sector experienced sea ice retreat during 1740–1770 and 1820–1840 [34]. Since the 1700s, a total expansion of $\sim 1.3^\circ$ has been estimated for the sea ice in the Amundsen and Ross seas [35]. Although these estimates of sea ice changes are generally in agreement, the considerable uncertainties arise from the individual proxies and different indicators employed, and the aforementioned reconstructions and their unified quantization require further validation [10,42].

Reconstructions of sea ice around Antarctica from regional to continental scales are essential to estimate the contribution of internal and external forcings in Antarctic sea ice variability and evaluate climate model simulations. To improve projections for the coming decades, an understanding of the interactions of teleconnections and local feedback mechanisms at longer time scales is needed. In this study, we use ice-core-based reconstructions to examine the regional and overall changes in Antarctic SIE during the past 100–200 years. We also discuss the possible mechanisms responsible for the identified variations in the context of climate variability at the multi-decadal scale.

2. Material and methods

2.1. Ice core data

In this study, we used ice core and fast-ice records with annual resolution from six sites to reconstruct the northernmost latitude of sea ice edge (NLSIE) for the following sectors of the Southern Ocean (Fig. 1). Preliminary identification of potential sectors was performed based on previous studies and the correlation between each proxy and the NLSIE for every 1° of longitude (Fig. S1 online). By enlarging or reducing the potential areas and calculating the correlations (Table S1 online) between the regional averaged NLSIE and the proxies, we selected the most extensive and significant ($\geq 95\%$ confidence level, CL) areas as the target sectors for reconstruction.

(1) The Weddell Sea (50°W – 20°E , hereafter referred to as WS). The NLSIE in WS was reconstructed using the South Orkney Fast-ice (SOFI) series as a proxy. The SOFI record is an annual record of fast-ice around the South Orkney Islands from 1903 to 2008. The day of continuous fast-ice formation, the timing of ice break-

out, and the duration of ice coverage have been correlated with the WS ice cover [43,44]. Our correlation analysis also showed that the fast-ice duration was significantly associated ($r = 0.6$, 99% CL) with the averaged NLSIE in the 50°W – 20°E longitudinal band from 1979 to 2008 (Fig. S1a and Table S1 online).

(2) The Bellingshausen Sea (50° – 90°W , hereafter referred to as BS). The NLSIE in BS was reconstructed using the annual net accumulation record from the Bruce Plateau ice core extracted from the Antarctic Peninsula, covering the period of 1900–2009 [41]. The accumulation rate exhibited a significant relationship ($r = -0.56$, 99% CL) with the averaged NLSIE in the 50° – 90°W longitudinal band during 1979–2009 (Fig. S1b and Table S1 online).

(3) The Amundsen Sea (90° – 140°W , hereafter referred to as AS). The NLSIE in AS was reconstructed using SOFI series, given its significant negative correlation ($r = -0.65$, 99% CL) with the averaged NLSIE in the 90° – 140°W longitudinal band (Fig. S1a and Table S1 online). Some studies have shown that the SOFI record represents sea ice change in the AS [42,44] in the context of the variability of the Antarctic Dipole.

(4) The Ross Sea (160°E – 140°W , hereafter referred to as RS). The NLSIE in RS was reconstructed using the MSA concentration derived from the Ferrigno and Erebus Saddle ice cores. The MSA concentration in the Ferrigno ice core was shown to be a robust proxy for winter SIE in RS for the period of 1703–2010 [35]. The MSA concentration in the Erebus Saddle ice core was used as a proxy to reconstruct the summer sea ice state in RS [45]. Our correlation analysis also suggested that the MSA concentrations in both the Erebus Saddle and Ferrigno demonstrated a good relationship with the NLSIE in RS (Fig. S1c, d online) and their leading principal component (PC1) was significantly correlated ($r = 0.6$, 99% CL) with the averaged NLSIE in the 140°W – 160°E longitudinal band since 1979 (Table S1 online).

(5) The Indian and western Pacific sector of the Southern Ocean (50° – 150°E , hereafter referred to as IndWPac). The NLSIE in IndWPac was reconstructed using MSA records obtained from the LGB69 [34] and Law Dome ice cores [30]. The LGB69 ice core covers 294 years, from 1708 to 2001, and the Law Dome ice core covers 155 years, from 1841 to 1995. The PC1 of the annual MSA concentration of the LGB69 and the Law Dome ice cores was significantly correlated ($r = 0.55$, 95% CL) with the averaged NLSIE in the 50° – 150°E longitudinal band during 1979–1995 (Fig. S1e, f and Table S1 online).

2.2. Validation of sea ice data

Satellite-derived sea ice concentration in the Antarctic has been used to evaluate the reconstructed sea ice variability since the beginning of the satellite era. These concentrations are derived from the Nimbus 7 Scanning Multichannel Microwave Radiometer, DMSP Special Sensor Microwave/Imager, and Special Sensor Microwave Imager and Sounder sensors [46]. The data have a spatial resolution of 25 km and cover the period from November 1978 to the present. The satellite-derived sea ice concentration is used to calculate the NLSIE, defined as the northernmost position of the 15% isopleth of the ice concentration for each degree of longitude.

2.3. Climate indices and reanalysis

The following climate indices are used to understand the potential role of large-scale modes of climate variability in the trends and multi-decadal variability of NLSIE in the different sectors of the Southern Ocean.

The Interdecadal Pacific Oscillation (IPO) is a measure of the decadal to interdecadal variability of the SST anomaly in the Pacific Ocean [47]. The index that tracks the IPO change is defined as the difference between SST anomalies averaged over the central

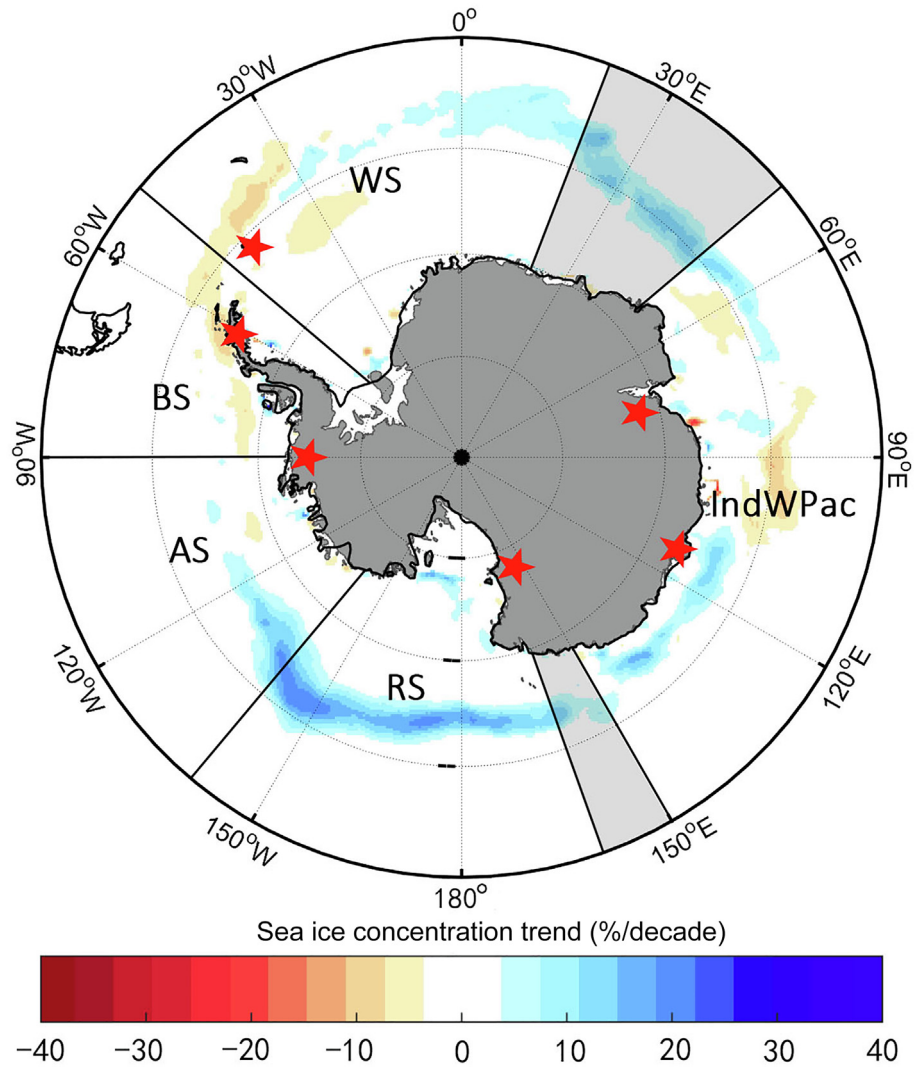


Fig. 1. Observed Antarctic sea ice concentration (colored area) trends for the extended winter season (August, September, and October) from 1979 to 2016. The red stars denote the proxy sites for sea ice reconstruction. The sectors are indicated as the Weddell Sea (WS), Bellingshausen Sea (BS), Amundsen Sea (AS), Ross Sea (RS), and Indian and western Pacific Ocean (IndWPac).

equatorial Pacific (10°S–10°N, 170°E–90°W) and averaged in the northwest (25°–45°N, 140°E–145°W) and southwest Pacific (50°–15°S, 150°E–160°W) [48]. The IPO index since 1854 can be found at the website of the NOAA Physical Sciences Laboratory (<http://www.esrl.noaa.gov/psd/data/timeseries/IPOTPI/>).

The Southern Annular Mode (also known as the Antarctic Oscillation) index is defined as the mean latitudinal difference in sea level pressure at 40° and 65°S; it is considered as the prevailing mode of atmospheric circulation in the Southern Hemisphere and explains about 35% of the extratropical Southern Hemisphere climate variability [49]. The SAM index since 1850 is available online (<http://ljp.gcess.cn/dct/page/65609>).

To facilitate the quantification of atmospheric circulation patterns associated with different phases of the aforementioned climate modes, we also used SST and 850 hPa wind field data from the European Centre for Medium-Range Weather Forecasts Interim Reanalysis (ERA-Interim; 1979 onwards) [50]. The reanalysis fields and the observed sea ice data were averaged for different phases of the climate indices to generate composite maps. Here we focus on August, September, and October (hereafter referred to as extended winter) because the maximum SIE typically occurs in September. In this study, the high (low) index years were identified as years

with greater (smaller) than one standard deviation. The final composite maps showed the differences between the years with high and low values of the climate indices. The statistical significance of the composites was assessed using the Student’s *t*-test.

We further used the data assimilation-based surface temperature reconstructions [51] to calculate the relationship between sea ice and surface temperature in the Antarctic. The mean surface temperature (MST) over the last two millennia was assimilated based on the new stable oxygen isotopes in ice cores compiled as part of the Antarctica2k framework [52]. The five Antarctic regions (i.e., Dronning Maud Land, Antarctic Peninsula, West Antarctic Ice Sheet, Victoria Land-Ross Sea, and Wilkes Land Coast) adjacent to the five relevant sectors were selected.

2.4. Reconstruction, calibration, and validation

Relationships between the proxies and sea ice data were investigated using linear regression and correlation analyses. The NLSIE was reconstructed using geometric mean regression (also known as reduced major axis regression) [32,35,53], which accounts for errors and noise in both the dependent and independent variables. For the IndWPac sector, the empirical orthogonal function (EOF)

analysis [54] was first used to calculate the PC1 of the MSA records from the LGB69 and Law Dome ice cores, and then the PC1 was used for the reconstruction, so as to maximize their association with NLSIE. The same procedure was applied to the RS sector, for which the MSA records from Ferrigno and Erebus Saddle ice cores were employed. The leave-one-out cross-validation method was used to verify the reconstruction results [55], and the transfer function in each sector was demonstrated to be valid. The uncertainty in each reconstruction was obtained by calculating the root mean square error (RMSE) based on the satellite record.

2.5. Time series analysis

Linear trends in the reconstructed NLSIE in all the five sectors were calculated via ordinary least squares slope estimation, and the significance level was estimated via a two-tailed Student's *t*-test. The method of sliding time windows was used to detect trend changes in the Antarctic composite NLSIE for various lengths of time. The sliding time windows used in this study ranged in length from 10 to 110 years.

A climatic regime shift is commonly deemed as a rapid reorganization of climate from one relatively stable state to another. Herein, we used a sequential data processing scheme developed by Rodionov [56,57] to identify the timing of possible regime shifts in the NLSIE time series. Multi-decadal shifts in mean conditions in the regional NLSIE were identified via a simple regime shift detection technique using shift detection v3-2 software.

We used multiple linear regression to estimate the degree to which the changes in the reconstructed NLSIE could be fitted by climate indices. Stepwise regression, which identified a useful subset of the predictors, was used. The MST, SAM, and IPO indices were selected as predictors. These indices were smoothed using a 31-year running average to extract the variability at the multi-decadal time-scale. To avoid multicollinearity, we identified the indices that were significantly correlated with the NLSIE. First, we selected the index with the largest correlation coefficient and examined its contribution to the NLSIE. Then, we selected one more index that had a significant correlation coefficient with the NLSIE, added it to the regression, and examined the joint contribution of the two indices. Finally, we assessed the relative contribution of each index in the multiple regression.

3. Results

3.1. Reconstructed NLSIE

The significant positive relationship ($r = 0.6$, 99% CL) between the SOFI record and the NLSIE in the WS sector allowed us to reconstruct the NLSIE back to 1903 (Fig. 2a, black line). The mean NLSIE in the WS sector was at 56.45°S during 1903–2007. Superimposed on strong interannual variability, the NLSIE has shown a significant decreasing trend (>95% CL) at a rate of -0.08° per decade since the 1900s. Regime shift analysis identified an abrupt change in the NLSIE in 1951 (Fig. 2a, blue line). The reconstruction of sea ice change in the WS sector was consistent with the estimates of summer SIE based on whaling records and ship logbooks [58,59], which indicated a decline in sea ice in the WS since the early 20th century.

The reconstructed NLSIE in the BS based on annual accumulation from the Bruce Plateau ice core was significantly correlated with the satellite-derived NLSIE from 1979 to 2009 ($r = -0.56$, 99% CL, Fig. 2b). Here the reconstructed NLSIE in the BS covers from 1900 to 2009 and extended from 50° to 90°W, which represented a larger sector than that estimated by Abram et al. [32] (70°–100°W) (Fig. 2b, black line). The mean NLSIE in the BS was at 61.83°S dur-

ing 1900–2009. Linear trend analysis for the entire period showed a significantly (99% CL) decreasing trend at a rate of -0.17° per decade. The decreasing trend of NLSIE is in agreement with other climate records and reconstructions [32,41,44]. A decreasing trend with regime shifts in 1978 and 1992 (Fig. 2b, blue line) means that the NLSIE in the BS has experienced accelerated retreat since the late 1970s.

The NLSIE in the AS sector from 1903 to 2007 (Fig. 2c, black line) was reconstructed according to the significant relationship between the SOFI record and the satellite-derived NLSIE in the AS sector from 140° to 90°W during 1979–2007 ($r = -0.65$, 99% CL). The mean NLSIE in the AS was at 65.02°S during the entire period of 1903–2007. A significant (95% CL) upward trend at a rate of $+0.08^\circ$ per decade was identified during the entire period, and a regime shift occurred in 1951 (Fig. 2c, blue line). The NLSIE variability in the AS was contrary to that in the WS sector, largely due to the Antarctic Dipole, which is a leading mode of Antarctic sea ice variability and usually exhibits an inverse relationship between the AS and WS [42].

The MSA records for both the Ferrigno and Erebus Saddle ice cores were significantly correlated with NLSIE in the RS from 1979 to 2006 (Fig. S1 online). To better interpret sea ice variability in the RS, the PC1 of the leading EOF mode for these two records was used for the NLSIE reconstruction (Fig. 2d, black line). The PC1 had a significant correlation with the satellite-derived NLSIE during 1979–2006 ($r = 0.6$, 99% CL, Fig. 2d). Here, the NLSIE spanned from 160°E to 140°W, which represented a much wider sector than that estimated in previous reconstructions [35,40]. The mean NLSIE in the RS was at 62.46°S during 1810–2006. Linear trend analysis for the entire period identified a significantly (99% CL) increasing trend at a rate of $+0.02^\circ$ per decade. The increasing trend agrees with previous reconstructions [35,40,42], which suggested a tendency toward more ice cover in the RS. The regime shifts occurred in 1840, 1876, 1933, 1947, and 1998. A stepwise increasing trend with regime shifts in 1947 and 1998 (Fig. 2d, blue line) means that the increasing NLSIE trend in the RS was accelerated to $+0.07^\circ$ per decade when calculated over the period spanning 1940s–2000s.

The NLSIE in the IndWPac sector since 1841 (Fig. 2e, black line) was reconstructed based on the significant correlation between the PC1 of the MSA records from the LGB69 and Law Dome ice cores and the satellite-derived NLSIE in the IndWPac during 1979–1995 ($r = 0.55$, 95% CL, Fig. 2e). The mean NLSIE in the IndWPac was at 59.51°S during 1841–1995. Superimposed on strong interannual variability, the NLSIE showed a significantly decreasing trend at a rate of -0.03° per decade (95% CL) over the entire period. The decrease in the NLSIE was not linear during 1841–1995, and the regime shifts occurred in 1930 and 1969. A remarkable retreat of sea ice has occurred since the late 1960s, and its mean NLSIE is 1.24 standard deviations lower than the NLSIE baseline (1841–1960) (Fig. 2e). The significant (95% CL) declining trend agrees with reconstructions published by Curran et al. [30] and Xiao et al. [34] and with whaling records [60] and reports of penguin populations [61], which suggest that sea ice reduced in the 1970s.

3.2. Potential drivers of NLSIE trends and multi-decadal variability

It is essential to understand the factors that caused the aforementioned changes in NLSIE for the past 100–200 years and how we can obtain insight sea ice anomalies during warm and cold periods. In the context of global warming, anomalies in atmospheric circulation are considered to be one of the important factors driving the increasing trend in Antarctic sea ice. It is well known that the SAM, which is generally related to the strength of the westerlies and Amundsen Sea Low, plays an important role in the dynamic processes of sea ice and climate in coastal

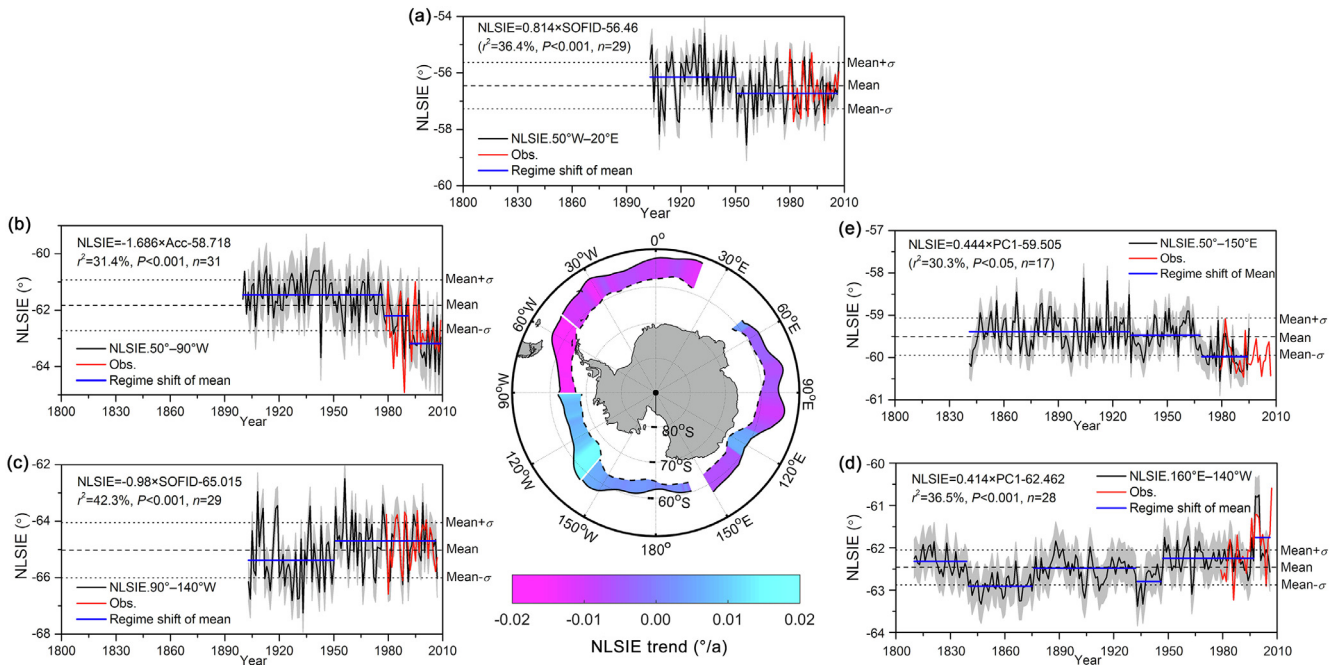


Fig. 2. Northernmost latitude of sea ice edge (NLSIE) reconstructions (black), regime shifts of mean (blue), satellite-derived NLSIE (red), and the associated uncertainty bands (± 1 RMSE, grey areas) for the WS (a), BS (b), AS (c), RS (d), and IndWPac (e) sectors. The horizontal dotted lines indicate standard deviation (σ) ranges around the baseline mean (entire period). The central map shows the reconstructed trends in the NLSIE (latitude per year) during the past 100–200 years.

Antarctica [11,62,63]. In response to a positive SAM trend observed since the mid-20th century [49,64], which is associated with the increased equatorward Ekman drift and warm poleward (cold equatorward) winds into the BS (RS) region, sea ice increases in the RS and decreases in the BS [10,62,65,66]. The IPO, an internally generated mode of climate variability, influences the Antarctic atmospheric circulation and sea ice with changes in the SST in the Pacific sector, specifically in the Ross, Amundsen, and Bellingshausen seas [14,15]. The negative trend in the IPO, with an average cooling of tropical Pacific SST and a deepening of the Amundsen Sea Low, accelerated the increasing trend in Antarctic sea ice between 2000 and 2014, particularly in the RS region [14]. However, the relationship between sea ice and regional temperature and the moderating role of atmospheric circulation at the multi-decadal scale is insufficiently understood. To investigate the potential drivers of the NLSIE trends and the multi-decadal sea ice variability described in Section 3.1, we compared the NLSIE series of the five sectors with surface temperature in coastal Antarctica and the indices (SAM and IPO) characterizing climate variability in the Southern Hemisphere. Conventionally, the average trend over a 30 year span is used to define the climatology. The NLSIE, MST, and climate indices were smoothed using a 31-year running average to remove high-frequency variations, emphasizing multi-decadal variability and long-term trends. Linearly detrended time series were further compared to analyze their behavior at the multi-decadal scale.

The NLSIE in the WS exhibited no significant relationship with the MST in Dronning Maud Land (Fig. 3a), whereas the decreasing trend in the NLSIE in the BS was consistent with the warming trend in the MST in the Antarctic Peninsula [67] during the 20th century (Fig. 3b). The rapid decrease in the NLSIE in the BS, which is close to the eastern margin of the Amundsen Sea Low, emerged after the 1950s and could be closely associated with the positive SAM [63,66]. Furthermore, the regime shifts of the NLSIE in the BS that occurred in the late 1970s and early 1990s were identified consistent with the positive shifts of the SAM [64]. We further used multiple regression to calculate the contribution rates of changes in the

SAM, IPO, and MST to the NLSIE variation (Table 1). The SAM, IPO, and MST together can explain 91.5% of the NLSIE in WS in terms of the long-term trend. The relative contributions of the SAM, IPO, and MST are 88.74%, 11.15%, and 0.11%, respectively. For the BS sector, the SAM, IPO, and MST together can explain 83.6% of the NLSIE long-term trend. The relative contributions of the SAM, IPO, and MST are 87.7%, 12.2%, and 0.1%, respectively. The results indicate that the long-term linear trend of the NLSIE in the WS and BS is mainly influenced by the SAM. Composite differences in SST, wind field, and the NLSIE anomalies between the high and low values of climate indices (Fig. 4) were obtained to further investigate the potential mechanisms. In the context of the positive SAM, the anomalous winds associated with the deepening of the Amundsen Sea Low (Fig. 4a, b) advect warm air to the BS and the Antarctic Peninsula [41,68,69]. The trend of warm air approaching the continent and the southward winds during the 20th century associated with the positive SAM might decrease sea ice in the BS and WS (Fig. 4c), and vice versa.

Changes in the NLSIE in RS are associated with the MST in the Victoria Land-Ross Sea during 1840s–1910s, when the SAM was neutral. In contrast, during periods in which the SAM was significantly positive (after the 1970s) or negative (1910s–1950s), changes in the NLSIE in the RS tend to be positively correlated with the SAM instead of the MST (Fig. 3d). Similar relationships were observed between the NLSIE in the AS, climate indices, and temperature in the West Antarctic Ice Sheet during the 20th century (Fig. 3c). The anti-phase relationship before the 1960s between the NLSIE and IPO indicates that the changes in the NLSIE might be partially attributed to the variation in the IPO (Fig. 3c). The SAM, IPO, and MST together can explain 81% and 93% of the variances in the long-term trends of the NLSIE in RS and AS, respectively. The relative contributions of the SAM to the NLSIE in the AS (87.31%) and RS (97.8%) are larger than those of the IPO and MST. The IPO plays a secondary role in the AS and its contribution rate is 10.97% (Table 1). Composite analyses suggest that the relatively cool (warm) SST in the south Pacific (Fig. 4a) and the strong northward (southward) winds from 140°W to 170°E (Fig. 4b) are

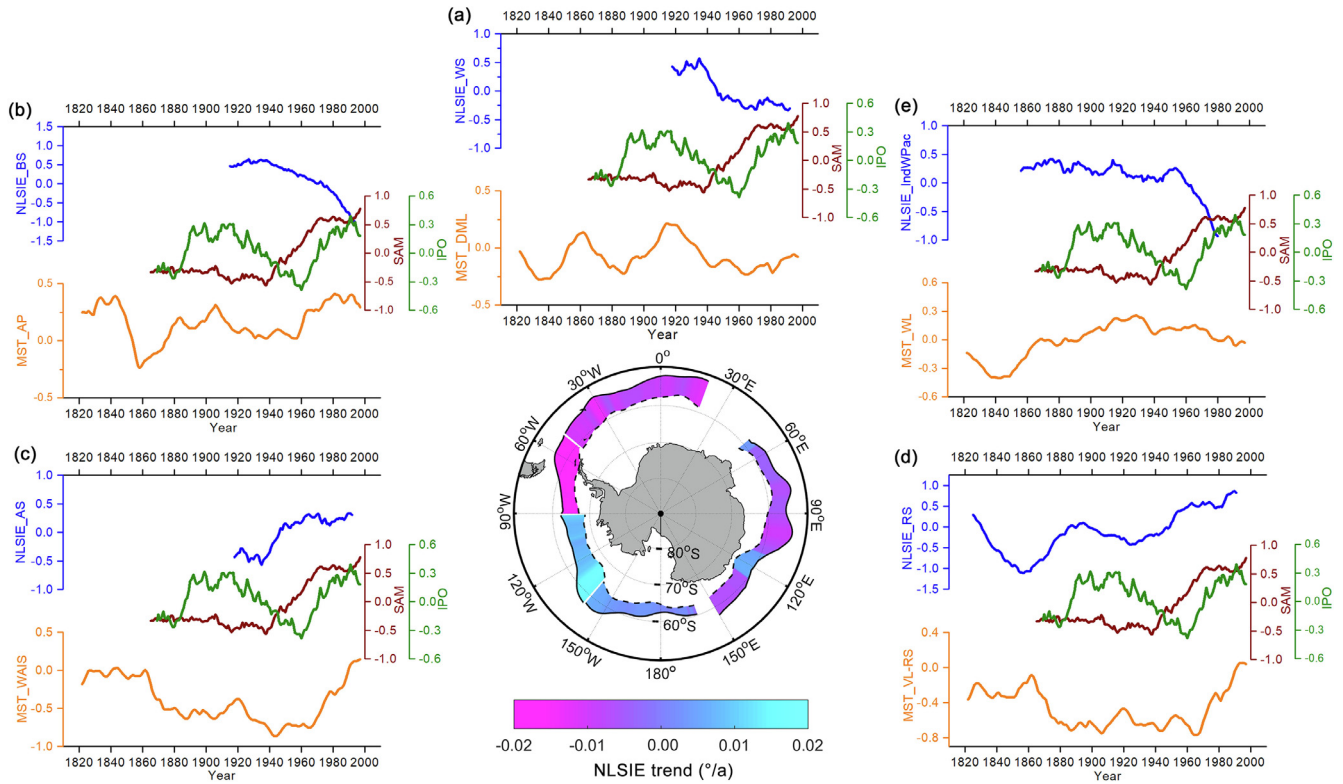


Fig. 3. Phasing of long-term variability over the past 100–200 years from proxy-derived indicators for the WS (a), BS (b), AS (c), RS (d), and IndWPac (e) sectors. Within each region (a–e), records were compiled as normalized data smoothed with a 31-year running average according to the parameter that they represent: NLSIE (blue), the extended winter (August, September, and October) mean Southern Annular Mode (SAM, wine) and Interdecadal Pacific Oscillation (IPO, green), and mean surface temperature (MST, orange; DML, AP, WAIS, VL–RS and WL means Dronning Maud Land, Antarctic Peninsula, West Antarctic Ice Sheet, Victoria Land–Ross Sea, and Wilkes Land Coast, respectively). The central map shows the reconstructed trends in the NLSIE (latitude per year) during the past 100–200 years.

Table 1

Contributions of the SAM, IPO and MST to the long-term trend of NLSIE during the past 100–200 years obtained by the multiple linear regression.

	Total explained variance (%)	Relative contribution of SAM (%)	Relative contribution of IPO (%)	Relative contribution of MST (%)
NLSIE_WS	91.5	88.74	11.15	0.11
NLSIE_BS	83.6	87.7	12.2	0.1
NLSIE_AS	93	87.31	10.97	1.72
NLSIE_RS	81	97.78	1.11	1.11
NLSIE_IndWPac	75.1	88.28	10.39	1.33

associated with the expansion (retreat) of the SIE in the Ross-Amundsen Sea (Fig. 4c) when the SAM is positive (negative).

There appears to be no significant relationship between the time series of the NLSIE in IndWPac and annual MST anomalies in the Wilkes Land coast sector (Fig. 3e). As shown in Fig. 3e, the relationship between the NLSIE in the IndWPac and the SAM was anti-phased at the multi-decadal scale, as the NLSIE retreats poleward when the SAM is positive. Multiple regression analysis shows that the SAM, IPO, and MST together can explain 75.1% of the variance in the trend of the NLSIE in IndWPac (Table 1). It is observed that the contribution of the SAM to the NLSIE in the IndWPac (88.28%) is greater than that of the IPO (10.39%). Composite analyses indicate that the strong westerlies in the IndWPac during the positive SAM phase (Fig. 4b) would limit SIE expansion (Fig. 4c).

Further detrending analyses (Fig. S2 and Table S2 online) show that the impact of the IPO on the NLSIE in the AS, BS, and WS increases (>60%), and this indicates that the multi-decadal oscillation of the NLSIE in these three sectors is mainly affected by the IPO. Although the impact of the IPO in the IndWPac sector has increased after detrending, the SAM still makes the largest contribution (>50%) to the NLSIE in the IndWPac. For the RS sector, the

multi-decadal oscillation of the NLSIE is primarily affected by the SAM, because the relative contribution rate is 100% after detrending. Previous studies involving composite analyses suggested that the same (inverse) phases of the SAM and IPO have contrary (similar) effects on the NLSIE in the AS to WS sector (Fig. 4c, f) by impacting the strength of the Amundsen Sea Low (Fig. 4b, e) [14,63,65]. Consistent with the increase in the meridional temperature gradient in the southern Pacific (Fig. 4d), the positive IPO produces an anomalous anticyclonic circulation (Fig. 4e). The anomalous southward winds in the AS suppress sea ice growth, whereas the anomalous northward winds in the BS and western WS are conducive to the increase in sea ice (Fig. 4f) during the positive IPO phase, and *vice versa*. These relationships are evidenced by the slowdown of the rate of increase (decrease) of the AS (WS) during the 1970s–1990s, when both the SAM and IPO were in the positive phase (Fig. S2a, c online).

Owing to the lack of SST proxy records, an important contribution of the SST to sea ice has not been discussed in this study. However, according to the only two long-term SST records obtained from the Antarctic Peninsula and the coast of George V Land, it can be inferred that the accelerated decreasing trends of the NLSIE

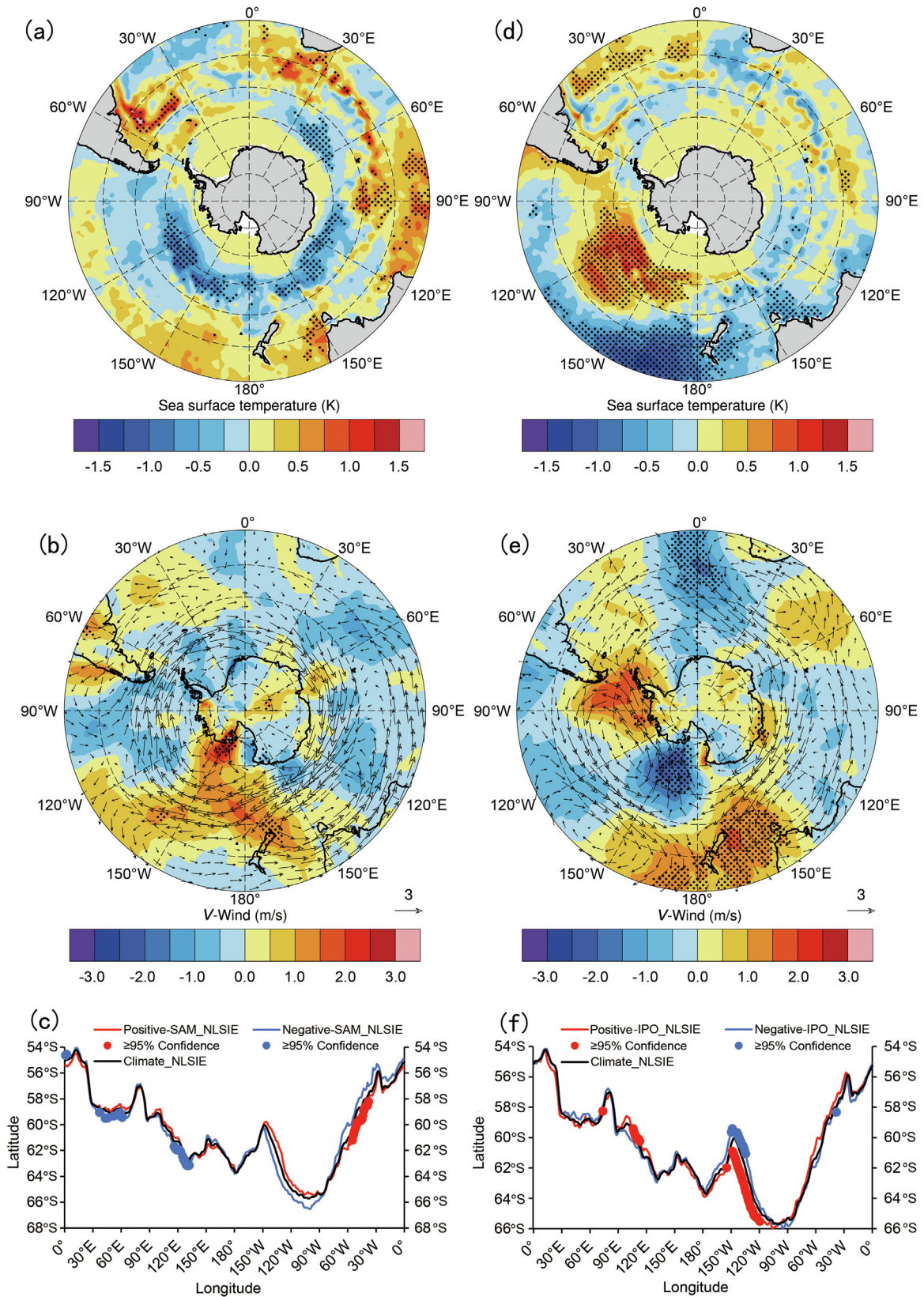


Fig. 4. Differences in the sea surface temperature (a, d), 850 hPa meridional wind (b, e, shaded), and NLSIE (c, f) for the extended winter (August, September, and October) season during the years of positive and negative SAM (a, b, c) and IPO (d, e, f). Values significant at the 95% level are stippled.

in the IndWPac and BS after the 1970s could be partly attributed to the increase in SST [70,71], and are the superposed results of the positive trend of the SAM [64] and SST [70]. The aforementioned results suggest that, over the last 200 years, changes in the extent of Antarctic sea ice during the extended winter were not forced solely by temperature or by atmospheric circulation, but rather by the combination of these factors.

3.3. Antarctic composite NLSIE trends during the 20th century

Although the current understanding of the historical sea ice variation in the Antarctic is not sufficient to reconstruct circum-Antarctic sea ice at the spatiotemporal scale over the past 200 years, our reconstructions, primarily based on various ice core proxies, could provide insight into sea ice variability for almost the entire Southern Ocean during the 20th century (Fig. 3). The total NLSIE in the Antarctic (hereafter NLSIE_Ant) was calculated as the weighted mean of the reconstructed composites in the five sectors. The resulting Antarctic NLSIE during the 20th century (1903–1995) after reconstruction is shown in Fig. 5a, along with the observed record

(1979–2016). The 11-a running average was used to compare the consistency in trends between the reconstructed and observed series without losing the decadal to multi-decadal variability. Overall, the decadal (11-a) mean of the NLSIE_Ant shows a significant decreasing trend (-0.03° per decade, 99% CL) during the whole time period and an increasing trend after the 1980s.

To further investigate the status of the observed increasing trend in the historical context, trends for NLSIE_Ant were calculated using differing start years and interval lengths (Fig. 5b). It should be noted that the data after 1979 in Fig. 5b are derived from observations. It was found that the significant decreasing in the NLSIE is incontrovertible if the start year was set no later than 1965 and a window length longer than 40 years was set. For time windows shorter than 40 years, the trend estimation values were positive during the 1930s–1940s and 1980s–2010s, and negative during the 1910s–1930s and 1950s–1970s. During the interval beginning from either year within 1981–1991, the sea ice extent demonstrated an increasing trend. In terms of its rate of increase and lifespan, the recent sea ice increase is unprecedented under the background of global warming.

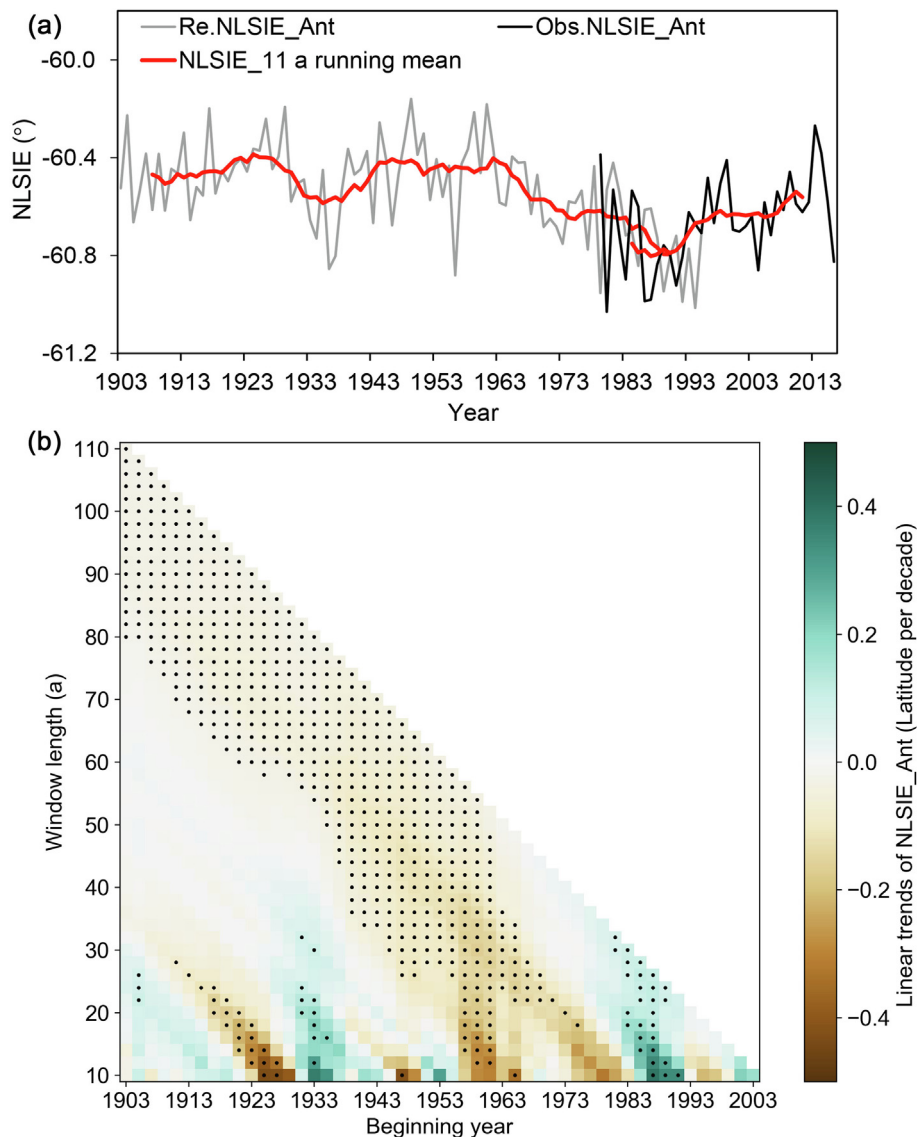


Fig. 5. (a) Reconstructed (gray) and satellite-derived (black) total NLSIE for the Antarctic (NLSIE_Ant) as annual (thin lines) and running decadal averages (red thick lines). (b) Trends for NLSIE_Ant with differing start years and interval lengths. All trends significant at the 95% level are stippled.

Combining the results in Section 3.2, we inferred that the decreasing trend of NLSIE_Ant during the 1955–1980 is dominated by the significant declines in the WS, BS, and IndWPac, which are primarily driven by the positive SAM and the SST warming in the coastal region of the Antarctic Peninsula and east Antarctica [72]. The significantly increasing trend from the early 1980s to the mid-2010s is dominated by the accelerated expansion of sea ice in the RS and AS, which is primarily driven by the anomalous northward winds associated with the positive SAM.

4. Conclusions

In this study, five ice cores and one fast ice record were revisited and used to reconstruct the NLSIE in the five sectors of the Southern Ocean. The MSA records from the LGB69 and Law Dome ice cores and those from the Erebus Saddle and Ferrigno ice cores are good proxies for the NLSIE in the IndWPac and RS, respectively. The snow accumulation record from the Bruce Plateau ice core is a good proxy for the NLSIE in the BS, and the SOFI record is useful for representing the NLSIE in the WS and AS sectors. All the reconstructed NLSIE trends capture a large portion of the observed NLSIE variability. Based on the analyses of the linear trend and regime shifts, our study reveals that the NLSIE in the IndWPac exhibited a significant (95% CL) decreasing trend at a rate of $+0.03^\circ$ per decade during the past 150 years, in which the most profound decline occurred during the late 1960s. In contrast, the NLSIE in the RS exhibited a significant (99% CL) increasing trend at a rate of $+0.02^\circ$ per decade during the past 200 years, in which the largest contribution comes from the last 60 years ($+0.07^\circ$ per decade during 1940–2006). In the AS, a significant (95% CL) increasing trend in the NLSIE has been observed since 1900 ($+0.07^\circ$ per decade), whereas the BS and WS exhibited a decreasing trend of -0.17° (99% CL) and -0.08° (95% CL) per decade during the 20th century, respectively. In both the AS and WS sectors, the NLSIEs indicate that a regime shift occurred in the early 1950s, whereas the regime shift occurred in late 1970s in the BS.

Compared with the climate indices and regional temperature records, our analyses suggest that the long-term linear trend of the NLSIE in each sector is significantly related to the SAM. The strengthened westerlies and Amundsen Sea Low, which are significantly associated with a positive SAM trend, result in sea ice retreat in the IndWPac, BS, and WS and in sea ice advance in the RS and AS. At the multi-decadal scale, the IPO plays a dominant role in the NLSIE variability in the AS, BS, and WS, whereas the contribution of the SAM is the largest in the IndWPac and RS. We infer that the multi-decadal forcing of the IPO might decelerate the rate of change of the NLSIE in the AS and WS, whereas the warming in the Indian Ocean and Antarctic Peninsula might accelerate the rate of retreat of the NLSIE in the IndWPac and BS from the late 20th century.

Our total composite NLSIE for the Antarctic shows a significant decreasing trend (-0.03° per decade, 99% CL) during the 20th century, and the rapid decline is detected during the period from 1955 to 1980. This suggests that the upward trend observed by satellites likely began in the early 1980s. When interpreting the recent increasing trend, the start point should be explicitly specified.

It should be noted that the results presented here may influence by potential uncertainty associated with the limited data used for the reconstruction and the analysis used to produce long-term climate indices. The ice-core-based sea ice reconstructions are usually limited by their dependence on favorable meteorological conditions (e.g., onshore winds). Thus, combining more available proxies from multiple archives is necessary to reduce the uncertainty produced by specific proxies and to investigate Antarctic sea ice variability at longer time scales and it links with climate modes. It is also necessary to further explore the mechanism of

sea ice changes at the multi-decadal scale in combination with climate models.

Conflict of interest

The authors declare that they have no conflict of interest.

Acknowledgments

This work was supported by the Strategic Priority Research Program of the Chinese Academy of Sciences (XDA19070103), the National Key Research & Development Program of China (2018YFA0605901), the State Key Laboratory of Cryospheric Science (SKLCS-ZZ-2021), and the National Natural Science Foundation of China (42071086, 41425003, 41941009). The authors are indebted to Elizabeth R. Thomas from British Antarctic Survey and Mark Curran from University of Tasmania for providing the Ferrigno and Law Dome MSA data. We gratefully acknowledge the other contributors who supplied the proxy data used in this study.

Author Contributions

Dahe Qin, Cunde Xiao and Jiping Liu contributed to overall framing of the study. Jiao Yang contributed to the drafting of this manuscript and the collection and analysis of data. Jiao Yang and Shutong Li contributed to implementation of methodology. Jiping Liu and Cunde Xiao contributed to interpretation of the results and revised the draft. All authors discussed the results and contributed to editing the manuscript.

Appendix A. Supplementary materials

Supplementary materials to this article can be found online at <https://doi.org/10.1016/j.scib.2021.07.028>.

References

- [1] Serreze MC, Meier WN. The Arctic's sea ice cover: trends, variability, predictability, and comparisons to the Antarctic. *Ann NY Acad Sci* 2019;1436:36–53.
- [2] Liu J, Chen Z, Hu Y, et al. Towards reliable Arctic sea ice prediction using multivariate data assimilation. *Sci Bull* 2019;64:63–72.
- [3] Intergovernmental Panel on Climate Change (IPCC). Summary for policymakers. In: Portner HO, Roberts DC, Masson-Delmotte V, editors. *the ocean and cryosphere in a changing climate*. IPCC special World Meteorological Organization; 2019.
- [4] Parkinson CL, Cavalieri DJ. Antarctic sea ice variability and trends, 1979–2010. *Cryosphere* 2012;6:871–80.
- [5] Hobbs WR, Bindoff NL, Raphael MN. New perspectives on observed and simulated Antarctic sea ice extent trends using optimal fingerprinting techniques. *J Clim* 2015;28:1543–60.
- [6] Turner J, Bracegirdle T, Phillips T, et al. An initial assessment of Antarctic sea ice extent in the CMIP5 models. *J Clim* 2013;26:1473–84.
- [7] Roach LA, Dörr J, Holmes CR, et al. Antarctic sea ice area in CMIP6. *Geophys Res Lett* 2020;47:e2019GL086729.
- [8] Chemke R, Polvani LM. Using multiple large ensembles to elucidate the discrepancy between the 1979–2019 modeled and observed Antarctic sea ice trends. *Geophys Res Lett*, 2020, 47: e2020GL088339
- [9] Matear RJ, O'Kane TJ, Risbey JS, et al. Sources of heterogeneous variability and trends in Antarctic sea-ice. *Nat Commun* 2015;6:8656.
- [10] Hobbs WR, Massom R, Stammerjohn S, et al. A review of recent changes in Southern Ocean sea ice, their drivers and forcings. *Glob Planet Change* 2016;143:228–50.
- [11] Liu J, Curry JA, Martinson DG. Interpretation of recent Antarctic sea ice variability. *Geophys Res Lett* 2004;31:L02205.
- [12] Li X, Holland DM, Gerber EP, et al. Impacts of the north and tropical Atlantic Ocean on the Antarctic Peninsula and sea ice. *Nature* 2014;505:538–42.
- [13] Kwok R, Comiso JC, Lee T, et al. Linked trends in the south pacific sea ice edge and Southern Oscillation index. *Geophys Res Lett* 2016;43:10295–302.
- [14] Meehl GA, Arblaster JM, Bitz CM, et al. Antarctic sea-ice expansion between 2000 and 2014 driven by tropical Pacific decadal climate variability. *Nat Geosci* 2016;9:590–5.

- [15] Purich A, England MH, Cai W, et al. Tropical Pacific SST drivers of recent Antarctic sea ice trends. *J Clim* 2016;29:8931–48.
- [16] Bintanja R, van Oldenborgh GJ, Drifflout SS, et al. Important role for ocean warming and increased ice-shelf melt in Antarctic sea-ice expansion. *Nat Geosci* 2013;6:376–9.
- [17] Swart NC, Fyfe JC. The influence of recent Antarctic ice sheet retreat on simulated sea ice area trends. *Geophys Res Lett* 2013;40:4328–32.
- [18] Purich A, England MH, Cai W, et al. Impacts of broad-scale surface freshening of the Southern Ocean in a coupled climate model. *J Clim* 2018;31:2613–32.
- [19] Armour KC, Marshall J, Scott JR, et al. Southern Ocean warming delayed by circumpolar upwelling and equatorward transport. *Nat Geosci* 2016;9:549–54.
- [20] Kostov Y, Ferreira D, Armour KC, et al. Contributions of greenhouse gas forcing and the southern annular mode to historical Southern Ocean surface temperature trends. *Geophys Res Lett* 2018;45:1086–97.
- [21] Stuecker MF, Bitz CM, Armour KC. Conditions leading to the unprecedented low Antarctic sea ice extent during the 2016 austral spring season. *Geophys Res Lett* 2017;44:9008–19.
- [22] Schlosser E, Haumann FA, Raphael MN. Atmospheric influences on the anomalous 2016 Antarctic sea ice decay. *Cryosphere* 2017;12:1103–19.
- [23] Meehl GA, Arblaster JM, Chung CTY, et al. Sustained ocean changes contributed to sudden Antarctic sea ice retreat in late 2016. *Nat Commun* 2019;10:14.
- [24] Purich A, England MH. Tropical teleconnections to Antarctic sea ice during austral spring 2016 in coupled pacemaker experiments. *Geophys Res Lett* 2019;46:6848–58.
- [25] Wang G, Hendon HH, Arblaster JM, et al. Compounding tropical and stratospheric forcing of the record low Antarctic sea-ice in 2016. *Nat Commun* 2019;10:13.
- [26] Goosse H, Lefebvre W, de Montety A, et al. Consistent past half-century trends in the atmosphere, the sea ice and the ocean at high southern latitudes. *Clim Dyn* 2009;33:999–1016.
- [27] Ding Q, Steig EJ, Battisti DS, et al. Winter warming in west Antarctica caused by central tropical Pacific warming. *Nat Geosci* 2011;4:398–403.
- [28] Bracegirdle TJ, Stephenson DB, Turner J, et al. The importance of sea ice area biases in 21st century multimodel projections of antarctic temperature and precipitation. *Geophys Res Lett* 2015;42:10832–9.
- [29] Thomas ER, Allen CS, Etourneau J, et al. Antarctic sea ice proxies from marine and ice core archives suitable for reconstructing sea ice over the past 2000 years. *Geosciences* 2019;9:506.
- [30] Curran MAJ, van Ommen TD, Morgan VI, et al. Ice core evidence for Antarctic sea ice decline since the 1950s. *Science* 2003;302:1203–6.
- [31] Becagli S, Castellano E, Cerri O, et al. Methanesulphonic acid (MSA) stratigraphy from a Talos Dome ice core as a tool in depicting sea ice changes and southern atmospheric circulation over the previous 140 years. *Atmos Environ* 2009;43:1051–8.
- [32] Abram NJ, Thomas ER, McConnell JR, et al. Ice core evidence for a 20th century decline of sea ice in the Bellingshausen sea Antarctica. *J Geophys Res* 2010;115:D23101.
- [33] Sneed SB, Mayewski PA, Dixon DA. An emerging technique: multi-ice-core multi-parameter correlations with Antarctic sea-ice extent. *Ann Glaciol* 2011;52:347–54.
- [34] Xiao C, Dou T, Sneed SB, et al. An ice-core record of Antarctic sea-ice extent in the southern Indian Ocean for the past 300 years. *Ann Glaciol* 2015;56:451–5.
- [35] Thomas ER, Abram NJ. Ice core reconstruction of sea ice change in the Amundsen-Ross seas since 1702 A.D. *Geophys Res Lett* 2016;43:5309–17.
- [36] Severi M, Becagli S, Caiazza L, et al. Sea salt sodium record from Talos Dome (east Antarctica) as a potential proxy of the Antarctic past sea ice extent. *Chemosphere* 2017;177:266–74.
- [37] Welch KA, Mayewski PA, Whitlow SI. Methanesulfonic acid in coastal Antarctic snow related to sea-ice extent. *Geophys Res Lett* 1993;20:443–6.
- [38] Curran MAJ, Jones GB. Dimethyl sulfide in the Southern Ocean: seasonality and flux. *J Geophys Res Atmos* 2000;105:20451–9.
- [39] Wolff EW, Fischer H, Fundel F, et al. Southern Ocean sea-ice extent, productivity and iron flux over the past eight glacial cycles. *Nature* 2006;440:491–6.
- [40] Sinclair KE, Bertler NAN, Bowen MM, et al. Twentieth century sea-ice trends in the Ross sea from a high-resolution, coastal ice-core record. *Geophys Res Lett* 2014;41:3510–6.
- [41] Porter SE, Parkinson CL, Mosley-Thompson E. Bellingshausen sea ice extent recorded in an Antarctic Peninsula ice core. *J Geophys Res* 2016;121:13886–900.
- [42] Hobbs W, Curran M, Abram N, et al. Century-scale perspectives on observed and simulated Southern Ocean sea ice trends from proxy reconstructions. *J Geophys Res Oceans* 2016;121:7804–18.
- [43] Mulvaney R, Wolff EW. Spatial variability of the major chemistry of the Antarctic ice sheet. *Ann Glaciol* 1994;20:440–7.
- [44] Murphy EJ, Clarke A, Abram NJ, et al. Variability of sea-ice in the northern Weddell sea during the 20th century. *J Geophys Res Oceans* 2014;119:4549–72.
- [45] Rhodes RH, Bertler NAN, Baker JA, et al. Sea ice variability and primary productivity in the Ross Sea, Antarctica, from methylsulphonate snow record. *Geophys Res Lett* 2009;36:L10704.
- [46] Cavalieri DJ, Parkinson CL, Gloersen P, et al. Data from “Sea ice concentrations from Nimbus-7 SMMR and DMSP SSM/I-SSMIS passive microwave data, Version 1.” NASA National Snow and Ice Data Center Distributed Active Archive Center. <https://nsidc.org/data/NSIDC-0051/versions/1>. (Accessed 31 December 2020).
- [47] Power S, Casey T, Folland C, et al. Inter-decadal modulation of the impact of ENSO on Australia. *Clim Dyn* 1999;15:319–24.
- [48] Henley BJ, Gergis J, Karoly DJ, et al. A tripole index for the Interdecadal Pacific Oscillation. *Clim Dyn* 2015;45:3077–90.
- [49] Marshall GJ. Trends in the Southern Annular Mode from observations and reanalyses. *J Clim* 2003;16:4134–43.
- [50] Dee DP, Uppala SM, Simmons AJ, et al. The ERA-Interim reanalysis: configuration and performance of the data assimilation system. *Q J R Meteorol Soc* 2011;137:553–97.
- [51] Klein F, Abram NJ, Curran MAJ, et al. Assessing the robustness of Antarctic temperature reconstructions over the past 2 millennia using pseudoproxy and data assimilation experiments. *Clim Past* 2019;15:661–84.
- [52] Stenni B, Curran MAJ, Abram NJ, et al. Antarctic climate variability on regional and continental scales over the last 2000 years. *Clim Past* 2017;13:1609–34.
- [53] Smith RJ. Use and misuse of the reduced major axis for line-fitting. *Am J Phys Anthropol* 2009;140:476–86.
- [54] Wilks DS. *Statistical methods in the atmospheric sciences*. 3rd ed. Amsterdam, Boston: Academic Press; 2011.
- [55] Michaelsen J. Cross-validation in statistical climate forecast models. *J Clim Appl Meteorol* 1987;26:1589–600.
- [56] Rodionov SN. Use of prewhitening in climate regime shift detection. *Geophys Res Lett* 2006;33:L12707.
- [57] Rodionov SN. A sequential algorithm for testing climate regime shifts. *Geophys Res Lett* 2004;31:111–42.
- [58] de la Mare WK. Changes in Antarctic sea-ice extent from direct historical observations and whaling records. *Clim Change* 2009;92:461–93.
- [59] Edinburgh T, Day JJ. Estimating the extent of Antarctic summer sea ice during the heroic age of Antarctic exploration. *Cryosphere* 2016;10:2721–30.
- [60] Mare WK. Abrupt mid-twentieth-century decline in Antarctic sea-ice extent from whaling records. *Nature* 1997;389:57–60.
- [61] Barbraud C, Weimerskirch H. Emperor penguins and climate change. *Nature* 2001;411:183–6.
- [62] Hosking JS, Orr A, Marshall GJ, et al. The influence of the Amundsen-Bellingshausen seas low on the climate of west antarctica and its representation in coupled climate model simulations. *J Clim* 2013;26:6633–48.
- [63] Raphael MN, Marshall GJ, Turner J, et al. The Amundsen Sea low: variability, change, and impact on Antarctic climate. *Bull Amer Meteorol Soc* 2016;97:111–21.
- [64] Yang J, Xiao C. The evolution and volcanic forcing of the Southern Annular Mode during the past 300 years. *Int J Climatol* 2018;38:1706–17.
- [65] Turner J, Hosking JS, Marshall GJ, et al. Antarctic sea ice increase consistent with intrinsic variability of the Amundsen sea low. *Clim Dyn* 2016;46:2391–402.
- [66] Holland MM, Landrum L, Kostov Y, et al. Sensitivity of Antarctic sea ice to the southern annular mode in coupled climate models. *Clim Dyn* 2017;49:1813–31.
- [67] Yao Y, Huang J, Luo Y, et al. An upgraded scheme of surface physics for Antarctic ice sheet and its implementation in the WRF model. *Sci Bull* 2016;61:576–84.
- [68] Clem KR, Fogt RL. Varying roles of ENSO and SAM on the Antarctic Peninsula climate in austral spring. *J Geophys Res Atmos* 2013;118:11481–92.
- [69] Turner J, Phillips T, Hosking JS, et al. The Amundsen Sea Low. *Int J Climatol* 2013;33:1818–29.
- [70] Jones JM, Gille ST, Goosse H, et al. Assessing recent trends in high-latitude southern hemisphere surface climate. *Nat Clim Chang* 2016;6:917–26.
- [71] Campagne P, Crosta X, Houssais MN, et al. Glacial ice and atmospheric forcing on the mertz glacier polynya over the past 250 years. *Nat Commun* 2015;6:6642.
- [72] Fan T, Deser C, Schneider DP. Recent Antarctic sea ice trends in the context of Southern Ocean surface climate variations since 1950. *Geophys Res Lett* 2014;41:2419–26.



Jiao Yang is a research associate of the State Key Laboratory of Cryospheric Science, Northwest Institute of Eco-Environment and Resources, Chinese Academy of Sciences. She received her Ph.D. degree in 2019 from the University of Chinese Academy of Sciences. Her research interest focuses on polar cryosphere and climate change, in particular natural climate variability and human-caused climate change impacts Polar Regions.



Cunde Xiao is a professor and the director of the State Key Laboratory of Earth Surface Processes and Resource Ecology, Beijing Normal University. His research interest focuses on cryosphere and global changes, cryosphere functions and their services. He is also serving as the coordinate leading author of Working Group I of Intergovernmental Panel on Climate Change (IPCC) sixth assessment report (AR6), and the secretary-general of China Society of Cryospheric Science.



Dahe Qin is a geographer, specialized in glaciology and climate change science. He is an academician of both the Chinese Academy of Sciences and the Third World Academy of Sciences. He has long been engaged in the cryosphere and global change research. He actively promotes the concept and to build a theoretical framework of the Cryospheric Science. He was the co-chairman of Working Group I of both AR4 and AR5, IPCC.